

DOI: 10.7522/j. issn. 1000-0240. 2021. 0023

FAN Yijiao, MA Xiaoyi, LIU Hui, et al. Climatic and environmental evolution during the Holocene in the eastern Arid Central Asia recorded by loess-paleosol sequences[J]. Journal of Glaciology and Geocryology, 2021, 43(3):818-826. [范义姣, 马箫忆, 刘慧, 等. 黄土记录的中亚干旱区东部全新世气候与环境演化[J]. 冰川冻土, 2021, 43(3):818-826.]

黄土记录的中亚干旱区东部全新世 气候与环境演化

范义姣¹, 马箫忆¹, 刘慧¹, 王树源¹, 杨军怀¹,
陈梓炫¹, 高福元², 贾佳³, 夏敦胜¹

(1. 兰州大学 资源环境学院 西部环境教育部重点实验室, 甘肃兰州 730000; 2. 兰州城市学院 地理与环境工程学院,
甘肃兰州 730070; 3. 浙江师范大学 地理与环境科学学院, 浙江金华 321004)

摘要: 选取位于中亚干旱区东部新疆天山地区的两个典型黄土沉积剖面, 通过磁学参数(χ_{ARM} /SIRM)、亮度(L^*)、有机碳/氮同位素($\delta^{13}C_{org}$ 和 $\delta^{15}N$)等记录, 对研究区内全新世以来的气候环境进行重建。结果表明:早全新世, χ_{ARM} /SIRM、 L^* 指示黄土成壤较弱、有机质含量低, $\delta^{13}C_{org}$ 记录表明区域降水较少, 共同反映该时期地表植被覆盖低、相对干旱的气候环境;中晚全新世, χ_{ARM} /SIRM、 L^* 和 $\delta^{13}C_{org}$ 记录的湿度逐渐增加, 黄土 $\delta^{15}N$ 偏正变化, 指示地表生态系统生产力增强、植被覆盖增加, 表明该区域气候适宜期发生在中晚全新世。中亚干旱区东部全新世以来的气候环境特征, 与北半球高纬度冰盖、太阳辐射强度的变化密切相关。

关键词: 黄土; $\delta^{13}C_{org}$; $\delta^{15}N$; 全新世; 新疆天山地区; 中亚干旱区东部

中图分类号: P532 **文献标志码:** A **文章编号:** 1000-0240(2021)03-0818-09

0 引言

新疆天山地区位于欧亚大陆内部、距离各大洋较远, 属于亚洲中部干旱区的重要组成部分。受地形地势的影响, 黄土多分布于河谷阶地和山前平原^[1], 如伊犁盆地、准噶尔盆地南缘和塔里木盆地北缘。新疆天山地区黄土研究对于揭示亚洲内陆干旱化、粉尘搬运堆积、大气环流和气候环境变化具有重要意义^[2-3]。

作为黄土研究中常用的气候代用指标, 磁学参数(χ_{ARM} /SIRM)和亮度(L^*)在黄土高原和中亚干旱区黄土古气候研究中得到了广泛的应用, 在指示成壤强度与有机质含量、揭示湿度演化方面具有重要意义^[4]。前人通过对全新世多个黄土沉积的磁学参数、亮度、粒度、地球化学等指标的对比研究, 指出中亚干旱区的湿度演化在中晚全新世以来呈现逐

渐增加的趋势^[5-6]。然而, 以上基于磁学参数、亮度等重建的黄土古气候研究仅集中于湿度演化, 关于区域植被和生态系统对相应气候环境的响应变化研究较少。土壤有机碳/氮同位素($\delta^{13}C_{org}$ 和 $\delta^{15}N$)主要来源于上覆植被的贡献^[7-9], 利用土壤中的碳/氮同位素组成可以重建古植被和古气候环境的演化。Rao等^[10]较早对伊犁盆地黄土 $\delta^{13}C_{org}$ 进行研究, 发现该区域至少在末次冰期以来都是由 C₃植物占据主导地位, 并根据地层与 $\delta^{13}C_{org}$ 变化的关系进一步提出该指标在重建降水方面具有较大潜力, 并得到了广泛的应用^[11-12]。此外, 来自黄土高原和西欧黄土研究表明土壤 $\delta^{15}N$ 组成在揭示地表生态系统环境变化与示踪方面具有重要指示意义^[13], 但是目前在中亚干旱区黄土中的应用较少, 这在一定程度上限制了人们对中亚干旱区东部地质历史时期的气

收稿日期: 2021-04-21; 修订日期: 2021-06-10

基金项目: 国家自然科学基金项目(41877444)资助

作者简介: 范义姣, 博士研究生, 主要从事第四纪黄土与气候变化研究. E-mail: fanyj18@lzu.edu.cn

通信作者: 夏敦胜, 教授, 主要从事环境磁学、干旱区环境及城市污染研究. E-mail: dsxia@lzu.edu.cn

候及生态环境响应的理解。

鉴于此,本文对新疆伊犁盆地KS16黄土剖面进行磁学、亮度和有机碳/氮同位素等多指标综合分析,结合天山北麓LJW10剖面已发表的 $\delta^{13}\text{C}_{\text{org}}$ 记录、同时测定该剖面的 $\delta^{15}\text{N}$ 指标,探讨了新疆天山地区地表植被和生态系统变化及其对气候环境的响应,旨在更好地理解中亚干旱区东部地区全新世时期的气候变化和生态环境的协同作用。

1 研究区与剖面概况

新疆天山位于中亚干旱区东部,黄土多呈条带状分布于天山北坡的山麓带和伊犁河谷的河流阶地上^[1]。该区域属于温带大陆性气候,常年受到西风控制:春夏季降水相对较多,主要来自西风环流携带的北大西洋及沿途湖泊水汽,部分水汽由北冰洋贡献;冬季受西伯利亚高压的影响,西风带北支向南移动导致降水较少^[14]。天山北部为准噶尔盆地,气候相对干旱,分布有广阔的沙漠和戈壁,为北坡黄土沉积提供潜在粉尘物源。从准噶尔盆地到天山北坡,气候呈现明显的垂直地带性分布,温度随海拔的升高逐渐降低,降水量相应地从150 mm逐

渐增加至500 mm^[15]。伊犁盆地气候相对湿润,开口向西的喇叭状地形有利于北大西洋水汽的长驱直入,受地形阻挡,西部平原地区降水量在200~500 mm之间,东部山区高达800 mm,年平均气温大约在2.6~9.2 °C之间^[16]。

本研究选取的KS16和LJW10剖面分别位于伊犁盆地东部和天山北坡(图1)。其中KS16剖面(43°25'56" N, 83°56'35" E, 海拔1314 m)厚2 m,上部0.3 m为古土壤层,下部1.7 m为黄土层。团队成员采用石英单片再生剂量法对14个光释光样品进行定年,建立的年代框架表明该剖面底部年代大致为12 ka,具体年代结果及年龄深度模型参见文献[17]。LJW10剖面(43°58'29" N, 85°20'10" E, 海拔1462 m)厚2.8 m,其中2.8 m~1.7 m为黄土沉积,1.7 m以上为全新世地层,又可以划分为黄土-古土壤亚层^[4,18]。Li等^[18]采用粗颗粒石英单片再生剂量法,结合中粒径和粗粒径钾长石红外激发后红外释光测年方法(post-IR IRSL)对该剖面进行定年研究,底部年代约为16 ka。前人对该剖面的磁学、亮度^[4],粒度^[19]以及有机碳同位素^[11]等进行了系统研究,本文主要对其 $\delta^{15}\text{N}$ 进行测定和分析。

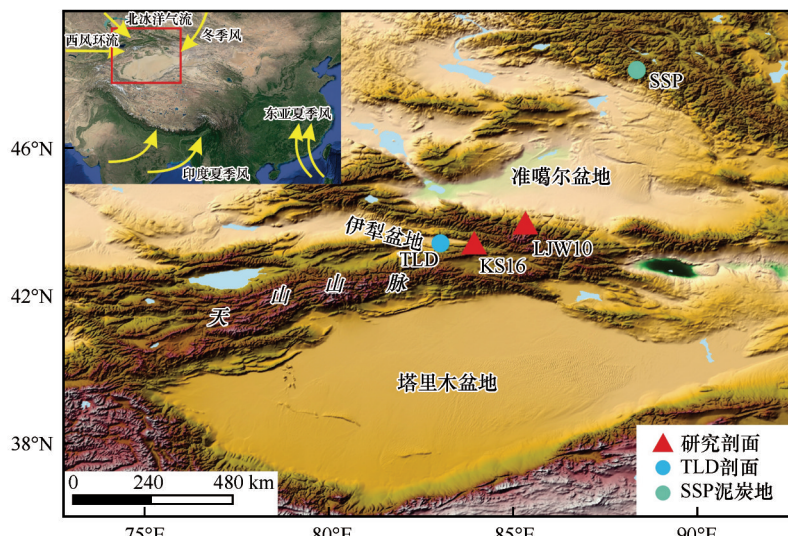


图1 研究区与剖面位置
Fig. 1 Study area and location of sections

2 实验方法

本研究对KS16剖面的磁学参数(χ_{ARM} 、SIRM)、亮度(L^*)以2 cm间隔进行测定,有机碳/氮同位素($\delta^{13}\text{C}_{\text{org}}$ 和 $\delta^{15}\text{N}$)以4 cm间隔测定;LJW10剖面 $\delta^{15}\text{N}$ 以4 cm间隔测定。磁学参数和亮度在兰州大学西部环境教育部重点实验室完成, $\delta^{13}\text{C}_{\text{org}}$ 和 $\delta^{15}\text{N}$ 在兰州大

学草地农业生态系统国家重点实验室完成。

非磁滞剩磁(ARM)是在直流磁场强度为0.05 mT叠加逐渐减弱的交变磁场(峰值为100 mT)后,使用Molspin Minispin小旋转磁力仪(JR-6A)测量,并换算为非磁滞剩磁磁化率(χ_{ARM});等温剩磁(IRM)使用ASCIM-10-30型脉冲强磁仪获得,样品在外加

1 T 磁场后使用 JR-6A 进行测量, 所获得的等温剩磁为饱和等温剩磁(SIRM)。亮度使用 X-Rite 948 型分光色度计量器, 将研磨至粉末的样品连续测试三次, 以保证误差小于 0.07。

$\delta^{13}\text{C}_{\text{org}}$ 和 $\delta^{15}\text{N}$ 测定之前, 采用酸洗法去除样品中碳酸盐部分^[11], 所有处理好的样品根据碳、氮含量确定称样量。使用装有连续进样装置的 Finnigan MAT253 稳定同位素质谱仪测定样品 $\delta^{13}\text{C}_{\text{org}}$ 和 $\delta^{15}\text{N}$, 测试过程中每隔 5 个样品加入 1 个标样[尿素标样, $\delta^{13}\text{C}_{\text{V-PDB}}=(-27.46\pm0.11)\text{\%e}$, $\delta^{15}\text{N}_{\text{AIR}}=(6.70\pm0.15)\text{\%e}$]确保仪器稳定、测试结果准确可靠。样品的 $\delta^{13}\text{C}_{\text{org}}$ 和 $\delta^{15}\text{N}$ 组成分别相对于 VPDB(Vienna Pee Dee Bellemnite) 和大气 N₂ 标准的千分之一(‰)变化。

3 各指标的气候环境指示意义

3.1 $\chi_{\text{ARM}}/\text{SIRM}$ 和 L^*

χ_{ARM} 能够灵敏反映磁性矿物中的单畴(SD)颗粒含量, SIRM 指示样品中亚铁磁性矿物和不完全反铁磁性矿物的含量^[20]。二者比值 $\chi_{\text{ARM}}/\text{SIRM}$ 通常被用于指示成壤作用, 高值表明较细磁性颗粒所占比例大, 成壤作用增强。亮度 L^* 反映土壤发育程度, 与有机质含量密切相关, L^* 值越低, 指示有机质含量较高, 进而反映区域植被覆盖和生物量^[21-22]。 $\chi_{\text{ARM}}/\text{SIRM}$ 和 L^* 指标已被广泛应用于恢复和重建干旱、半干旱地区的气候环境演化^[4-5]。

3.2 $\delta^{13}\text{C}_{\text{org}}$

土壤有机质主要来源于上覆植被, 因此黄土 $\delta^{13}\text{C}_{\text{org}}$ 很大程度依赖于上覆植被 $\delta^{13}\text{C}$ ^[23-24]。陆地植被主要分为 C₃、C₄ 和 CAM 植物, 其中 C₃ 植物 $\delta^{13}\text{C}$ 位于 -22‰~ -32‰, 平均值为 -27‰, C₄ 植物 $\delta^{13}\text{C}$ 位于 -9‰~ -19‰, 均值为 -13‰^[25]。植物在进行光合作用过程中, 碳同位素分馏很大程度受气候的影响, 根据 Farquhar 等^[26]提出的 C₃ 植物 $\delta^{13}\text{C}$ 分馏模式, 在相对潮湿的条件下, C₃ 植物的 $\delta^{13}\text{C}$ 通常更偏负, 因为在湿润环境中 C₃ 植物的气孔导度相对较高, 进而增加细胞间的 CO₂ 分压, 导致 $\delta^{13}\text{C}$ 值偏负; 在干旱条件下, 植物为了维持水分供应关闭气孔, 使得植物的气孔导度低, 植物叶片细胞间的 CO₂ 浓度降低, 植物固定 CO₂ 能力减弱, 最终导致植物 $\delta^{13}\text{C}$ 值升高。因此植被 $\delta^{13}\text{C}$ 变化与水分条件密切相关, 大量的现代植被和表土 $\delta^{13}\text{C}_{\text{org}}$ 研究发现中亚干旱区主要由 C₃ 植物占据主导地位, 并且 $\delta^{13}\text{C}_{\text{org}}$ 与降水量之间呈现明显的负相关性^[11-12, 27-28], 这一关系被广泛应用于该区

域降水量的重建^[11-12, 29], 并得到数值模拟结果的支持^[11]。此后, 中亚干旱区黄土 $\delta^{13}\text{C}_{\text{org}}$ 多用于讨论区域湿度的演化, 如新疆天山地区 LJW10^[11]、TLD 剖面^[30], 伊朗 YE 剖面^[29]和哈萨克斯坦 VA 剖面^[31] $\delta^{13}\text{C}_{\text{org}}$ 记录都表明中亚干旱区中晚全新世湿度逐渐增加(图 2)。因此, 本研究将 $\delta^{13}\text{C}_{\text{org}}$ 作为区域降水量变化的指标, 进而指示湿度演化。

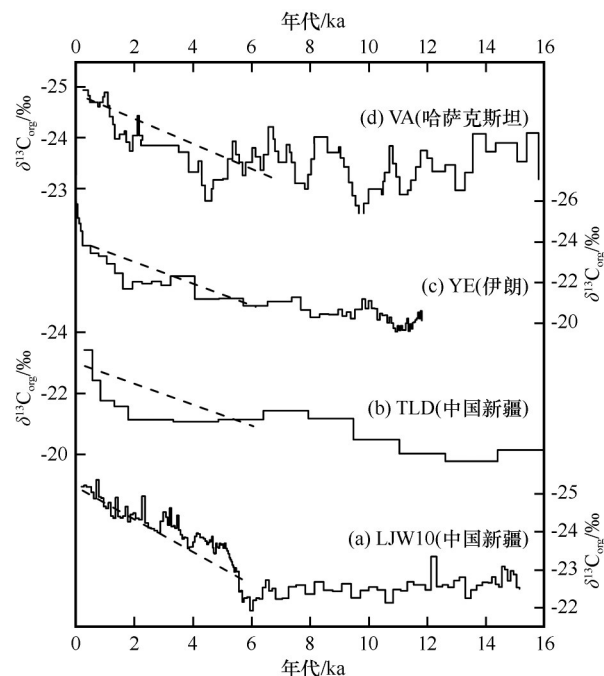


图 2 中亚干旱区黄土 $\delta^{13}\text{C}_{\text{org}}$ 记录对比

Fig. 2 The comparison of loess $\delta^{13}\text{C}_{\text{org}}$ records in arid Central Asia

3.3 $\delta^{15}\text{N}$

中亚干旱区关于土壤 $\delta^{15}\text{N}$ 与气候环境之间的现代过程研究几乎空白, 无法区分单一的温度、降水对土壤 $\delta^{15}\text{N}$ 的影响。尽管在全球尺度上, 上覆植被及土壤 $\delta^{15}\text{N}$ 与温度呈正相关、与降水量呈反相关^[32], 但这一关系存在区域差异性: 如黄土高原地区, 现代植被和表土 $\delta^{15}\text{N}$ 随降水量的增加逐渐偏负^[13]; 而在年均降水量小于 600 mm 的草原生态系统中, 土壤 $\delta^{15}\text{N}$ 随降水量的增加逐渐偏正^[33]。由于缺少区域现代过程的研究, 土壤 $\delta^{15}\text{N}$ 无法用于重建单一气候因子的变化。但是, 黄土高原西峰^[8]和渭南^[9]剖面, 西欧 Belotinac^[34]、Tokaj^[35] 和 Crvenka^[36] 等剖面黄土 $\delta^{15}\text{N}$ 研究都表明, 间冰期和相对暖湿的环境与 $\delta^{15}\text{N}$ 高值相对应, 同时生态系统生产力相对提高以及氮循环相对开放, 而冰期和相对冷干的环境则相反(图 3)。因此, 本研究将土壤 $\delta^{15}\text{N}$ 作为指示地表生态系统生产力的指标, 进而反映区域环境演化。

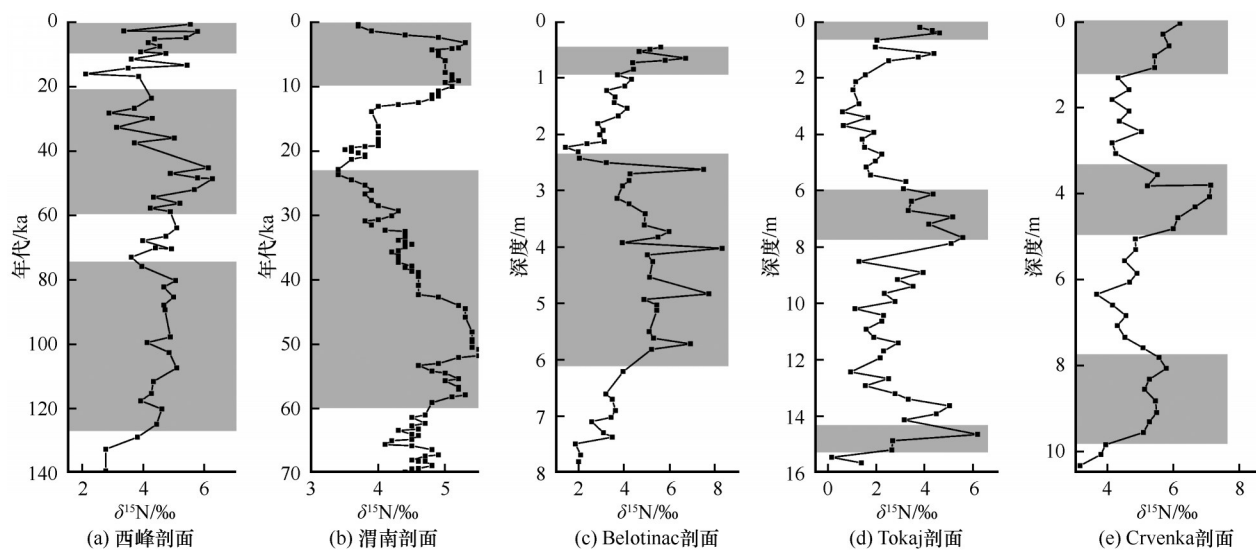


图3 黄土高原^[8-9](a, b)和西欧^[34-36](c, d, e)黄土-古土壤序列 $\delta^{15}\text{N}$ 变化(灰色阴影表示间冰期和暖湿期)

Fig. 3 Variation of $\delta^{15}\text{N}$ of loess-paleosol sequences in Chinese Loess Plateau^[8-9] (a, b) and Western Europe^[34-36] (c, d, e)
(The grey shaded areas represent interglacial and warm-humid periods)

4 结果与分析

4.1 $\chi_{\text{ARM}}/\text{SIRM}$ 和 L^*

如图4所示, KS16剖面 $\chi_{\text{ARM}}/\text{SIRM}$ 与 χ_{lf} 、 χ_{fd} ^[15] 变化较为一致, 峰谷变化整体与地层对应[图4(a)~(c)]。在 2.0~1.0 m, $\chi_{\text{ARM}}/\text{SIRM}$ 值较低, 在

6.73×10⁻⁵~11.6×10⁻⁵ mA⁻¹ 之间变化; 1.0 m 以上地层尤其是 0.6 m 以上, $\chi_{\text{ARM}}/\text{SIRM}$ 逐渐增大, 指示成壤作用增强。KS16剖面 L^* 在 53.7~70.5 之间变化[图4(d)], 与磁学指标的变化相似, 从 0.6 m 开始 L^* 值逐渐降低, 说明有机质含量逐渐增加。

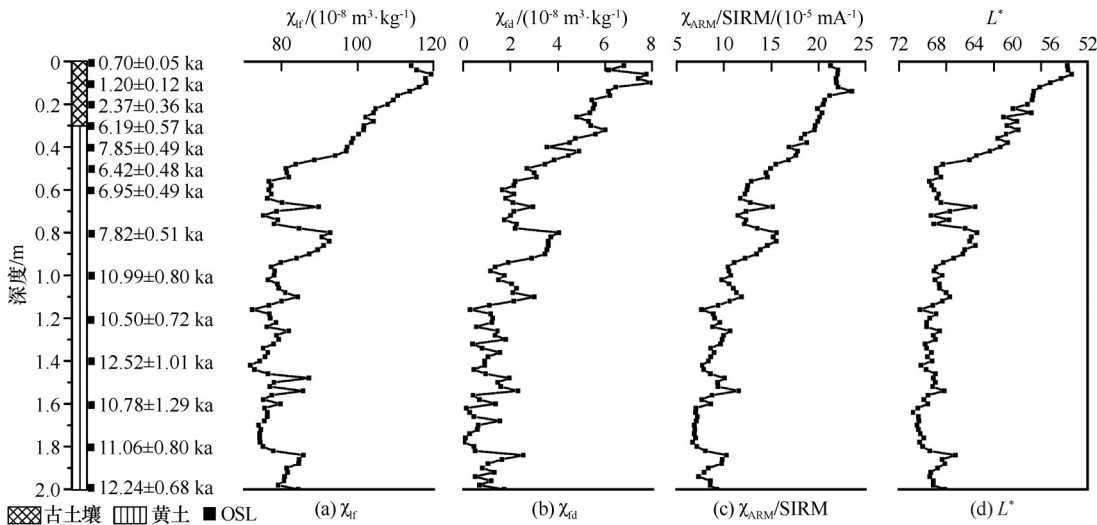


图4 KS16剖面地层和磁学参数、亮度变化(年代结果、 χ_{lf} 和 χ_{fd} 来自文献[17])

Fig. 4 Stratigraphy and variation of magnetic parameters and lightness on KS16 section
(The age results, χ_{lf} and χ_{fd} were modified from Reference [17])

4.2 $\delta^{13}\text{C}_{\text{org}}$ 和 $\delta^{15}\text{N}$

如图5(a)所示, KS16剖面 $\delta^{13}\text{C}_{\text{org}}$ 在 -25.31‰~ -22.68‰ 之间波动, 均值为 -23.43‰, 表明 C_3 植物占据主导。下部地层 $\delta^{13}\text{C}_{\text{org}}$ 整体波动较小, 0.6 m 以上的 $\delta^{13}\text{C}_{\text{org}}$ 与 $\chi_{\text{ARM}}/\text{SIRM}$ 、 L^* 变化一致, 越往上部地层

越偏负; 该剖面 $\delta^{15}\text{N}$ 在 2.15‰~5.00‰ 之间变化, 均值为 4.00‰, 整体呈现偏正的变化趋势。LJW10剖面 $\delta^{15}\text{N}$ 在 3.63‰~7.14‰ 之间变化, 均值为 5.49‰, 下部 2.0~1.7 m 黄土层 $\delta^{15}\text{N}$ 值最低, 1.5 m 以上地层黄土 $\delta^{15}\text{N}$ 逐渐偏正[图5(b)]。需要指出的是, 由于地

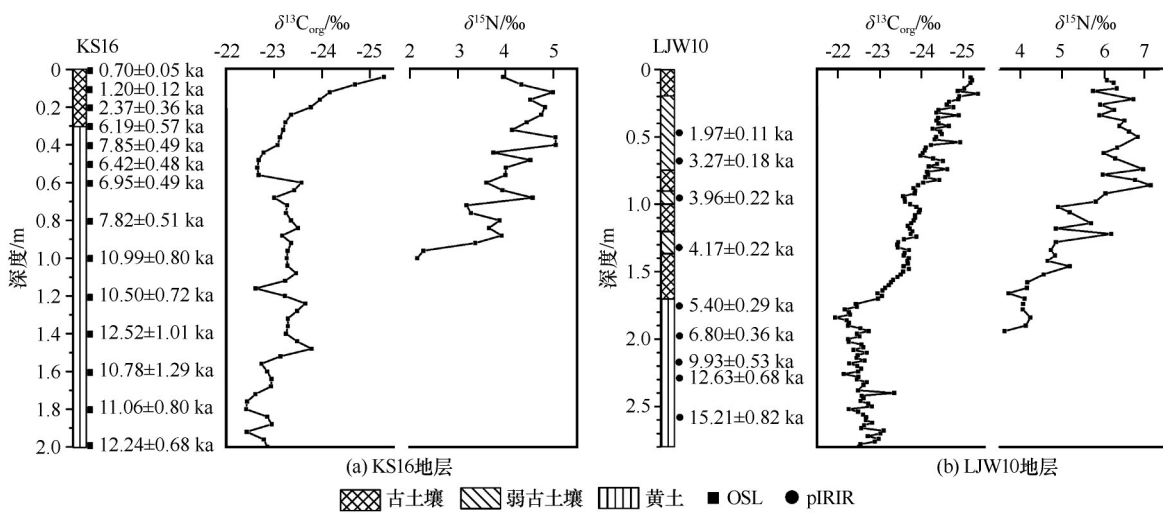


图 5 KS16 和 LJW10 剖面地层与 $\delta^{13}\text{C}_{\text{org}}$ 、 $\delta^{15}\text{N}$ 变化 (KS16 剖面年代来自文献[17], LJW10 剖面年代来自文献[18]、 $\delta^{13}\text{C}_{\text{org}}$ 来自文献[11])

Fig. 5 Stratigraphy and variations of $\delta^{13}\text{C}_{\text{org}}$ and $\delta^{15}\text{N}$ on KS16 and LJW10 sections (The ages of KS16 are from Reference [17], the ages and $\delta^{13}\text{C}_{\text{org}}$ of LJW10 section are from Reference [18] and Reference [11], respectively)

层下部样品氮含量特别低,导致仪器无法准确测定土壤 $\delta^{15}\text{N}$,因此 KS16 剖面仅测定上部 1 m, LJW10 剖面测定上部 1.7 m。

5 全新世气候与环境演化

为了更好地理解新疆天山地区气候环境演变及其与中亚干旱区和北半球高纬地区气候的联系,将本研究的结果与周边区域及北半球高纬度记录进行对比讨论(图 6)。KS16 剖面黄土 $\delta^{13}\text{C}_{\text{org}}$ 在 $-22.5\text{‰} \sim -25.5\text{‰}$ 之间变化,尽管植物凋落、腐烂、埋藏过程中会发生 1‰ 的分馏^[37],剖面 $\delta^{13}\text{C}_{\text{org}}$ 记录仍然表明全新世期间该区域植被由 C_3 植物主导。根据 $\delta^{13}\text{C}_{\text{org}}$ 与降水量的关系,早全新世时期 $\delta^{13}\text{C}_{\text{org}}$ 相对高值指示低降水量,而在中晚全新世逐渐偏负的 $\delta^{13}\text{C}_{\text{org}}$ 则指示降水相应增加[图 6(c)]。两个剖面 $\delta^{15}\text{N}$ 记录都表现为偏正变化趋势,指示中晚全新世地表生态系统生产力增强[图 6(d)~(e)]。结合 KS16 剖面各指标的变化,早全新世 $\chi_{\text{ARM}}/\text{SIRM}$ 、 L^* 、 $\delta^{13}\text{C}_{\text{org}}$ 记录的低湿度表明此时新疆天山地区气候相对冷干,有机质和植被覆盖度低、成壤微弱;中晚全新世, $\chi_{\text{ARM}}/\text{SIRM}$ 、 L^* 和 $\delta^{13}\text{C}_{\text{org}}$ 记录的湿度显著增加,同时 $\delta^{15}\text{N}$ 呈现偏正变化[图 6(a)~(d)],指示相对开放的地表生态系统生产力,说明该区域在湿度增加背景下,植被覆盖增多、有机质含量增加、成壤增强。尽管两个剖面下部地层的 $\delta^{15}\text{N}$ 无法测定,但间接反映当时气候环境整体干旱,地表植被覆盖度低,生态系统生产力较弱,土壤氮含量较低;中晚全

新世,在温度^[38]和湿度^[39]增加的背景下[图 6(g)~(h)],地表植被环境改善,生态系统生产力和氮循环开放程度相应增强,土壤 $\delta^{15}\text{N}$ 逐渐偏正变化,这也进一步说明该区域气候适宜期出现在晚全新世^[40~41]。

新疆天山其他地区黄土记录的全新世气候环境与本研究的结果较为一致:Duan 等^[42]基于天山北麓多个黄土剖面及地层年代结果发现古土壤形成时期主要发生在晚全新世,基于烧失量反映的碳酸盐含量及粒度端元模型分离出来的西风组分的变化都指示全新世以来呈现逐渐湿润的趋势;陆生蜗牛化石数量能够反映植被生态及蜗牛生存环境,早全新世的蜗牛化石数量较低而在晚全新世达到最高值[图 6(f)],逐渐偏负变化的 $\delta^{13}\text{C}_{\text{org}}$ 和显著增加的烧失量都表明晚全新世湿润的气候环境为蜗牛生长提供适宜的生存环境和充足的食物来源^[30];Kang 等^[6]对该区域多个黄土剖面的磁化率、粒度参数的分析,发现中晚全新世有效湿度逐渐增加。此外,多个黄土剖面的各项环境指标进一步证实新疆天山地区黄土沉积记录了中晚全新世湿度环境的增强^[4,19,41],有利于古土壤发育、植被覆盖增加及地表生态系统生产力的增强。

本研究中黄土沉积记录的区域环境呈现早全新世期间相对干旱,中晚全新世湿度逐渐增加的特征。Chen 等^[4,43]结合地质记录与数值模拟,认为早全新世较强的夏季太阳辐射[图 6(j)],使得温度升高,加速北半球高纬度地区剩余冰盖的撤退与融化

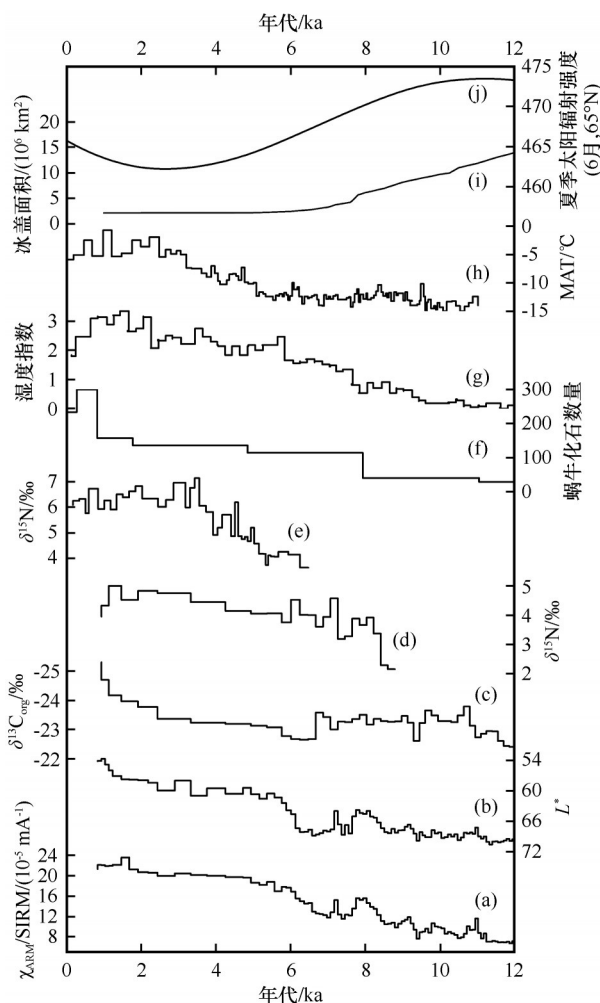


图6 两个剖面记录的全新世气候环境(a-d为KS16剖面记录,e为LJW10剖面记录)与区域及北半球记录对比(f为TLD剖面蜗牛化石总数^[30],g为新疆区域湿度集成曲线^[38],h为基于阿尔泰山泥炭 α -纤维素 $\delta^{13}\text{C}$ 重建的温度曲线^[39],i为北半球高纬度冰盖面积变化^[44],j为北半球高纬度太阳辐射^[45])

Fig. 6 Regional climatic environment during the Holocene recorded by two loess sections (a-d are records from KS16 section, e is from LJW10 section) and their comparison with regional and northern hemisphere records (f is the total count fossils from TLD section^[30], g is the synthesis of moisture changes in Xinjiang region^[38], h is the reconstructed temperature variation from the peat α -cellulose $\delta^{13}\text{C}$ of Altai Mountains^[39], i is the variation of northern hemisphere high-latitude ice sheets in million km²^[44], j is the northern hemisphere summer insolation^[45])

[图6(i)],大量冰融水进入北大西洋进而抑制表层水汽的蒸发;而相对较弱的冬季太阳辐射使中-高纬度之间的经向温度梯度减小,降低西风环流的强度,同时该区域上风向的水体(地中海、里海和黑海)蒸发减弱,导致西风环流携带至新疆天山地区的水汽减少。此外,外部边界条件(大气 CO_2)以

及较强的夏季太阳辐射使得该区域地表蒸发增强^[47]对早全新世干旱环境也有重要影响。相反,在中晚全新世北半球高纬度冰盖基本融化的背景下,随着夏季太阳辐射的减弱和冬季太阳辐射的增强,较强的西风环流携带更多水汽致使该区域降水增加^[43],为生物、植被生长和土壤发育提供充足条件,因此这一时期普遍发育古土壤,地表植被覆盖增加且生态系统生产力增强。

6 结论

本研究以新疆天山地区的KS16和LJW10黄土剖面为研究对象,结合常规指标($\chi_{\text{ARM}}/\text{SIRM}$ 、 L^*)和 $\delta^{13}\text{C}_{\text{org}}$ 、 $\delta^{15}\text{N}$ 记录对研究区内全新世气候环境进行重建。研究结果表明:早全新世, $\chi_{\text{ARM}}/\text{SIRM}$ 、 L^* 与 $\delta^{13}\text{C}_{\text{org}}$ 记录表明成壤较弱,植被覆盖少,有机质含量低,说明该时期呈现相对干旱的气候环境;中晚全新世,偏正变化的 $\delta^{15}\text{N}$ 指示地表生态系统生产力增强,植被覆盖增多,与 $\chi_{\text{ARM}}/\text{SIRM}$ 、 L^* 和 $\delta^{13}\text{C}_{\text{org}}$ 记录的湿度增加近乎同步,反映该区域处于全新世适宜期。本研究结果与区域其他黄土剖面记录的全新世气候环境演化相一致,表现为早全新世相对干旱,中晚全新世湿度逐渐增加、地表生态系统生产力增强,这种气候环境演化特征与北半球高纬冰盖面积、太阳辐射强度的变化密切相关。

谨以此文,纪念李吉均院士!

参考文献(References):

- [1] Ye Wei, Sang Changqing, Zhao Xingyou. Spatial-temporal distribution of loess and source of dust in Xinjiang [J]. Journal of Desert Research, 2003, 23(5): 514-520. [叶玮, 桑长青, 赵兴有. 新疆黄土分布规律及粉尘来源[J]. 中国沙漠, 2003, 23(5): 514-520.]
- [2] Song Yougui, Lai Zhongping, Li Yun, et al. Comparison between luminescence and radiocarbon dating of late Quaternary loess from the Ili Basin in Central Asia [J]. Quaternary Geochronology, 2015, 30: 405-410.
- [3] Li Jijun. The patterns of environmental changes since late Pleistocene in northwestern China [J]. Quaternary Sciences, 1990, 10(3): 197-204. [李吉均. 中国西北地区晚更新世以来环境变迁模式[J]. 第四纪研究, 1990, 10(3): 197-204.]
- [4] Chen Fahu, Jia Jia, Chen Jianhui, et al. A persistent Holocene wetting trend in arid Central Asia, with wettest conditions in the late Holocene, revealed by multi-proxy analyses of loess-paleosol sequences in Xinjiang, China [J]. Quaternary Science Reviews, 2016, 146: 134-146.
- [5] Gao Fuyuan, Jia Jia, Xia Dunsheng, et al. Assessment of the dominant climatic factor affecting pedogenic development in eolian sequences during the Holocene in arid Central Asia [J]. Quaternary International, 2019, 502: 78-84.
- [6] Kang Shugang, Wang Xulong, Roberts H M, et al. Increasing

- effective moisture during the Holocene in the semiarid regions of the Yili Basin, Central Asia: evidence from loess sections [J]. *Quaternary Science Reviews*, 2020, 246: 106553.
- [7] Hatté C, Antoine P, Fontugne M, et al. $\delta^{13}\text{C}$ of loess organic matter as a potential proxy for paleoprecipitation [J]. *Quaternary Research*, 2001, 55(1): 33-38.
- [8] Liu Junchi, Liu Weiguo. Soil nitrogen isotopic composition of the Xifeng loess-paleosol sequence and its potential for use as a paleoenvironmental proxy [J]. *Quaternary International*, 2017, 440: 35-41.
- [9] Liu Jiangsi, Algeo T J, Yang Huan, et al. Changes in vegetation type on the Chinese Loess Plateau since 75 ka related to East Asian summer monsoon variation [J]. *Palaeogeography, Palaeoclimatology, Palaeoecology*, 2018, 510: 124-139.
- [10] Rao Zhiguo, Xu Yuanbin, Xia Dunsheng, et al. Variation and paleoclimatic significance of organic carbon isotopes of Ili loess in arid Central Asia [J]. *Organic Geochemistry*, 2013, 63: 56-63.
- [11] Xie Haichao, Zhang Huiwen, Ma Jianying, et al. Trend of increasing Holocene summer precipitation in arid Central Asia: evidence from an organic carbon isotopic record from the LJW10 loess section in Xinjiang, NW China [J]. *Palaeogeography, Palaeoclimatology, Palaeoecology*, 2018, 509: 24-32.
- [12] Wang Qiang, Wang Xin, Wei Haitao, et al. Climatic significance of the stable carbon isotopic composition of surface soils in northern Iran and its application to an early Pleistocene loess section [J]. *Organic Geochemistry*, 2019, 127: 104-114.
- [13] Liu Weiguo, Wang Zheng. Nitrogen isotopic composition of plant-soil in the Loess Plateau and its responding to environmental change [J]. *Chinese Science Bulletin*, 2009, 54(2): 272-279. [刘卫国, 王政. 黄土高原现代植物-土壤氮同位素组成及对环境变化的响应 [J]. 科学通报, 2008, 53(23): 2917-2924.]
- [14] Aizen V B, Aizen E M, Joswiak D R, et al. Climatic and atmospheric circulation pattern variability from ice-core isotope/geochemistry records (Altai, Tien Shan and Tibet) [J]. *Annals of Glaciology*, 2006, 43(1): 49-60.
- [15] Zhang Jianxin, Liao Feijia, Zhang Lei. Evaluation of the effect of evaporation on water capacity of precipitation in the north slope of the middle Tianshan Mountains [C]// Proceedings of 2006 annual meeting of Chinese Meteorological Society: symposium on weather modification technology. Beijing: China Meteorological Society, 2006: 21-23. [张建新, 廖飞佳, 张磊. 中天山北坡蒸发对降水产水能力影响的评估 [C]// 中国气象学会2006年年会“人工影响天气作业技术专题研讨会”分会场论文集. 北京: 中国气象学会, 2006: 21-23.]
- [16] Ye Wei. Characteristics of physical environment and conditions of loess formation in Yili area, Xinjiang [J]. *Arid Land Geography*, 1999, 22(3): 9-16. [叶玮. 新疆伊犁地区自然环境特点与黄土形成条件 [J]. 干旱区地理, 1999, 22(3): 9-16.]
- [17] Jia Jia, Chen Jianhui, Wang Zhiyuan, et al. No evidence for an anti-phased Holocene moisture regime in mountains and basins in Central Asian: records from Ili loess, Xinjiang [J]. *Palaeogeography, Palaeoclimatology, Palaeoecology*, 2021, 572: 110407.
- [18] Li Guoqiang, Wen Lijuan, Xia Dunsheng, et al. Quartz OSL and K-feldspar pIRIR dating of a loess/paleosol sequence from arid Central Asia, Tianshan Mountains, NW China [J]. *Quaternary Geochronology*, 2015, 28: 40-53.
- [19] Jia Jia, Liu Hao, Gao Fuyuan, et al. Variations in the westerlies in Central Asia since 16 ka recorded by a loess section from the Tien Shan Mountains [J]. *Palaeogeography, Palaeoclimatology, Palaeoecology*, 2018, 504: 156-161.
- [20] Evans M E, Heller F. Magnetism of loess/palaeosol sequences: recent developments [J]. *Earth-Science Reviews*, 2001, 54(1/2/3): 129-144.
- [21] Sun Youbin, He Liu, Liang Lianji, et al. Changing color of Chinese loess: geochemical constraint and paleoclimatic significance [J]. *Journal of Asian Earth Sciences*, 2011, 40(6): 1131-1138.
- [22] Yang Shiling, Ding Zhongli. Color reflectance of Chinese loess and its implications for climate gradient changes during the last two glacial-interglacial cycles [J]. *Geophysical Research Letters*, 2003, 30(20): 2058.
- [23] Hatté C, Fontugne M, Rousseau D D, et al. $\delta^{13}\text{C}$ variations of loess organic matter as a record of the vegetation response to climatic changes during the Weichselian [J]. *Geology*, 1998, 26(7): 583-586.
- [24] Liu Weiguo, Yang Hong, Ning Youfeng, et al. Contribution of inherent organic carbon to the bulk $\delta^{13}\text{C}$ signal in loess deposits from the arid western Chinese Loess Plateau [J]. *Organic Geochemistry*, 2007, 38(9): 1571-1579.
- [25] Deines P. The isotopic composition of reduced organic carbon [M]// Fritz P, Fontes J Ch. *Handbook of environmental isotope geochemistry: the terrestrial environment A*. New York: Elsevier, 1980: 339-345.
- [26] Farquhar G D, Ehleringer J R, Hubick K T. Carbon isotope discrimination and photosynthesis [J]. *Annual Review of Plant Physiology and Plant Molecular Biology*, 1989, 40(1): 503-537.
- [27] Lee Xinqing, Feng Zhaodong, Guo Lanlan, et al. Carbon isotope of bulk organic matter: a proxy for precipitation in the arid and semiarid Central Asia [J]. *Global Biogeochemical Cycles*, 2005, 19(4): GB4010.
- [28] Rao Zhiguo, Guo Wenkang, Cao Jiantao, et al. Relationship between the stable carbon isotopic composition of modern plants and surface soils and climate: a global review [J]. *Earth-Science Reviews*, 2017, 165: 110-119.
- [29] Wang Qiang, Wei Haitao, Khormali F, et al. Holocene moisture variations in western arid Central Asia inferred from loess records from NE Iran [J]. *Geochemistry, Geophysics, Geosystems*, 2020, 21(3): e2019GC008616.
- [30] Zong Xiulan, Dong Jibao, Cheng Peng, et al. Terrestrial mollusk records in the loess sequences from eastern Central Asia since the last deglaciation and their paleoenvironmental significance [J]. *Palaeogeography, Palaeoclimatology, Palaeoecology*, 2020, 556: 10980.
- [31] Ran Min, Feng Zhaodong. Variation in carbon isotopic composition over the past ca. 46,000 yr in the loess-paleosol sequence in central Kazakhstan and paleoclimatic significance [J]. *Organic Geochemistry*, 2014, 73: 47-55.
- [32] Amundson R, Austin A T, Schuur E, et al. Global patterns of the isotopic composition of soil and plant nitrogen [J]. *Global Biogeochemical Cycles*, 2003, 17(1): 1031.
- [33] Zhou Lei, Song Minghua, Wang Shaoliang, et al. Patterns of soil $\delta^{15}\text{N}$ and total N and their relationships with environmental factors on the Qinghai-Tibetan Plateau [J]. *Pedosphere*, 2014, 24(2): 232-242.
- [34] Obreht I, Buggle B, Catto N, et al. The late Pleistocene Belotinac section (southern Serbia) at the southern limit of the European loess belt: environmental and climate reconstruction using grain size and stable C and N isotopes [J]. *Quaternary International*

- tional, 2014, 334(17): 10-19.
- [35] Schatz A-K, Zech M, Buggle B, et al. The late Quaternary loess record of Tokaj, Hungary: reconstructing palaeoenvironment, vegetation and climate using stable C and N isotopes and biomarkers [J]. *Quaternary International*, 2011, 240 (1) : 52-61.
- [36] Zech R, Zech M, Marković S, et al. Humid glacials, arid interglacials? Critical thoughts on pedogenesis and paleoclimate based on multi-proxy analyses of the loess-paleosol sequence Crvenka, Northern Serbia[J]. *Palaeogeography, Palaeoclimatology, Palaeoecology*, 2013, 387: 165-175.
- [37] Wang Guo'an, Feng Xiaohong, Han Jiamao, et al. Paleovegetation reconstruction using $\delta^{13}\text{C}$ of soil organic matter[J]. *Biogeosciences*, 2008, 5: 1325-1337.
- [38] Wang Wei, Feng Zhaodong. Holocene moisture evolution across the Mongolian Plateau and its surrounding areas: a synthesis of climatic records [J]. *Earth-Science Reviews*, 2013, 122: 38-57.
- [39] Wu Dandan, Cao Jiantao, Jia Guodong, et al. Peat brGDGTs-based Holocene temperature history of the Altai Mountains in arid Central Asia [J]. *Palaeogeography, Palaeoclimatology, Palaeoecology*, 2020, 538: 109464.
- [40] Gao Fuyuan, Jia Jia, Xia Dunsheng, et al. Asynchronous Holocene climate optimum across mid-latitude Asia [J]. *Palaeogeography, Palaeoclimatology, Palaeoecology*, 2019, 518: 206-214.
- [41] Sun Huanyu, Song Yougui, Chen Xiuling, et al. Holocene dust deposition in the Ili Basin and its implications for climate variations in Westerlies-dominated Central Asia [J]. *Palaeogeography, Palaeoclimatology, Palaeoecology*, 2020, 550: 109731.
- [42] Duan Futao, An Chengbang, Wang Wei, et al. Dating of a late Quaternary loess section from the northern slope of the Tianshan Mountains (Xinjiang, China) and its paleoenvironmental significance[J]. *Quaternary International*, 2020, 544: 104-112.
- [43] Chen Fahu, Chen Jianhui, Huang Wei, et al. Westerlies Asia and monsoonal Asia: spatiotemporal differences in climate change and possible mechanisms on decadal to sub-orbital timescales[J]. *Earth-Science Reviews*, 2019, 192: 337-354.
- [44] Dalton A S, Margold M, Stokes C R, et al. An updated radio-carbon-based ice margin chronology for the last deglaciation of the North American Ice Sheet Complex[J]. *Quaternary Science Reviews*, 2020, 234: 106223.
- [45] Laskar J, Robutel P, Joutel F, et al. A long-term numerical solution for the insolation quantities of the Earth [J]. *Astronomy and Astrophysics*, 2004, 428(1): 261-285.
- [46] Long Hao, Shen Ji, Chen Jianhui, et al. Holocene moisture variations over the arid Central Asia revealed by a comprehensive sand-dune record from the central Tian Shan, NW China [J]. *Quaternary Science Reviews*, 2017, 174: 13-32.
- [47] Zhang Xiaojian, Jin Liya, Chen Jie, et al. Detecting the relationship between moisture changes in arid Central Asia and East Asia during the Holocene by model-proxy comparison[J]. *Quaternary Science Reviews*, 2017, 176: 36-50.

Climatic and environmental evolution during the Holocene in the eastern Arid Central Asia recorded by loess-paleosol sequences

FAN Yijiao¹, MA Xiaoyi¹, LIU Hui¹, WANG Shuyuan¹, YANG Junhuai¹,
CHEN Zixuan¹, GAO Fuyuan², JIA Jia³, XIA Dunsheng¹

(1. Key Laboratory of Western China's Environmental Systems, Ministry of Education, College of Earth and Environmental Sciences, Lanzhou University, Lanzhou 730000, China; 2. College of Geography and Environmental Engineering, Lanzhou City University, Lanzhou 730070, China; 3. College of Geography and Environmental Sciences, Zhejiang Normal University, Jinhua 321004, Zhejiang, China)

Abstract: Two typical loess-paleosol sequences (KS16 and LJW10), located in the Tianshan region of Xinjiang in the eastern Arid Central Asia (ACA), were selected to reconstruct the climatic and environmental evolution during the Holocene. The susceptibility parameters (χ_{ARM} /SIRM), lightness (L^*), organic carbon/nitrogen isotope ($\delta^{13}C_{org}$ and $\delta^{15}N$) of the KS16 section ($43^{\circ}25'56''N, 83^{\circ}56'35''E$, 1 314 m a. s. l.) in the Ili Basin were analyzed comprehensively. In addition, we combined the $\delta^{15}N$ of LJW10 section ($43^{\circ}58'29''N, 85^{\circ}20'10''E$, 1 462 m a. s. l.), located in the northern Tianshan Mountains, and the proxies (χ_{ARM} /SIRM, L^* , $\delta^{13}C_{org}$, $\delta^{15}N$,) of KS16 section to reconstruct regional climatic and environmental evolution during the Holocene, which is helpful to understanding the synergistic effects of climate change and ecological environment in the eastern Arid Central Asia. The results show that: During the early Holocene, the χ_{ARM} /SIRM and L^* both indicated the pedogenesis was relatively weak and the organic matter content was low in the loess, with positive $\delta^{13}C_{org}$ showed regional precipitation was limited, which reflected the low vegetation coverage and relatively arid climate environment during this period. During the middle and late Holocene, the variations of χ_{ARM} /SIRM, L^* and $\delta^{13}C_{org}$ showed the moisture gradually increased, and the $\delta^{15}N$ record presented more positive, which all indicated that the climatic optimum occurred at this period. The climatic and environmental characteristics of the eastern Arid Central Asia during the Holocene are closely related to the variations of the high latitude ice sheet and the intensity of insolation in northern hemisphere.

Key words: loess; $\delta^{13}C_{org}$; $\delta^{15}N$; Holocene; Tianshan region of Xinjiang; eastern Arid Central Asia

(责任编辑: 赵井东; 编辑: 武俊杰)